Thermodynamic Investigation on the Mn-V-O Oxide System and Gibbs Energy of Formation of MnV_2O_4 Spinel Solid Solution

Min-Su Kim[1,], Youn-Bae Kang[1], Hae-Geon Lee[1] and Woo-Yeol Cha[2]*

1) Graduate Institute of Ferrous Technology, Pohang University of Science and Technology, Pohang, Rep. of Korea

2) Steelmaking Research Group, Technical Research Laboratories, POSCO, Pohang, Rep. of Korea

Abstract: As the first step of thermodynamic investigation on the Mn-V-O oxide system, phase equilibria of the Mn-V-O systems under controlled atmosphere have been experimentally investigated in the temperature range from 1200 to 1600°C and in the range of $\log p_{O_2}$ from -6 to -13. The following phases have been observed; molten oxide, manganosite (MnO (s.s.)), spinel (MnV_2O_4 (s.s.)), and vanadium trioxide (V_2O_3 (s.s.)). It was found in the present study that oxygen partial pressure has a significant effect on sub-solidus phase equilibria, in particular for solubility limit of intermediate phase (e.g., MnV_2O_4 (s.s.)). Once the phase equlibria of the Mn-V-O system was obtained, a subsequent thermodynamic investigation for the MnV_2O_4 spinel phase was followed to measure the Gibbs energy of formation of the spinel phase employing chemical equilibration technique. The standard Gibbs free energy of formation of the MnV_2O_4 spinel phase was calculated from the equilibrium compositions of elements in liquid iron or liquid copper, and thermodynamic parameters available in the literatures. From the information obtained in the present study, a stability diagram of Fe-Mn-V-O system was constructed which can be used as an inclusion stability diagram.

Key words: phase equilibria, Mn-V-O system, spinel, standard Gibbs free energy, MnV_2O_4.

1. Introduction

Manganese and vanadium are considered as typical alloying elements in many steel grades or deoxidizer. Due to their stronger affinity to oxygen than Fe, Mn and V in steel could react with dissolved oxygen to form complex oxide phases as inclusions. Such inclusions remained in the steel may play an important role to the properties of the steel products, or some of those may be absorbed into mold flux during continuous casting, thus those inclusions may affect the casting performance.

In order to understand and control the formation of such inclusions, it is indispensable to have in-depth knowledge in phase equilibria and thermodynamics of the complex inclusion system. Unfortunately, there has been only a little information available on phase equilibria of the Mn-V-O system. Furthermore, information under reducing condition relevant to steelmaking process is very rare.

Both manganese and vanadium are transition metals and they could take several different valences in oxides; Mn^{2+}, $Mn^{3+,}$ Mn^{4+}, V^{2+}, V^{3+}, V^{4+} and V^{5+} depending on temperature, oxygen partial pressure prevailing in the system and phase where they exist. It is well known that, under a moderately reducing condition, Mn^{2+} is dominant among other different valence states in its oxide form of MnO[1]. On the other hand, V seems to be stable as V^{3+} in solid oxide (*i.e.* V_2O_3) under oxygen partial pressure of steelmaking [2].

The first step of the present study is to experimentally investigate phase equilibria in the Mn-V-O oxide system under various oxygen partial pressure and temperatures relevant to steelmaking process condition. After obtaining thermodynamic information in the Mn-V-O oxide system, the stability of the intermediate phase will be studied by the measurement of standard Gibbs energy of formation of the intermediate phase and attainment of the stability diagram of the Fe-Mn-V-O system.

2. Phase equilibria in the Mn-V-O system

2.1 Experimental

The MnO (99.9% purity, Kosundo, Japan) and V_2O_3 directly reduced from V_2O_5 powder (orange color, 99.0% purity, Daejung chemicals) using H_2 (99.99% purity) gas in the laboratory, both in powder form, were mixed in the desired composition and ground by ball-milling under ethyl alcohol for 8 hr and dried at 70°C. Each sample of different compositions was weighted 1g, pelletized and placed in a boat made by folding Mo foil (0.1mm thickness) or Pt crucible (OD: 10mm, h: 12mm, t: 0.1mm) depending on oxygen partial pressure and temperature in each experiment. The sample was then placed in the uniform temperature zone of an alumina tube which was equipped with a vertical $MoSi_2$ resistance furnace. The alumina tube was tightly sealed by water-cooled brass end cap. Temperature was continuously monitored through each runs using a B type Pt/Rh thermocouple placed immediately above the sample.

The oxygen partial pressure was controlled by flowing a proper CO/CO_2 gas mixture or CO_2/H_2 gas mixture. Moistures in CO and CO_2 gases were removed by passing over $CaSO_4$ and CO_2 impurities in CO gas was purified by passing through sodium hydroxide (Ascarite®). Total flow rate was 400mL/min and mass flow controllers for CO, CO_2, and H_2 gas were preliminarily calibrated using soap-bubble-column technique.

The temperature for the present investigation was set between 1200°C and 1600°C. Each sample was placed in the furnace for 1 day (at 1600°C) or heated 100°C higher than the desired temperature for 1 hour before 3-day equilibration (at the temperatures lower than 1600°C). After equilibration, the sample was quenched rapidly into ice water. Portion of each sample was then mounted in epoxy resin, and polished for examination by EPMA.

The EPMA was carried out on a JEOL 8100-JXA in the WDS mode. Data were reduced using ZAF correction routine. For standards, pure MnO crystals supplied from JEOL Ltd. and V_2O_3 prepared by the present authors were used for manganese and vanadium concentrations. At least ten analyses were made of each phase in a sample and were averaged. The standard deviation of the measurement was within 1 mass pct in most cases. The crystal structures of phases observed in the samples were confirmed by the XRD analysis which was carried out using a Bruker AXS D8 Advance X-ray diffractometer with Cu-Kα radiation.

Attainment of equilibrium was assured by same final phases and compositions with different starting compositions and well grown facets of crystals. At least one common final equilibrium assemblages starting from different initial compositions in each run were confirmed.

The EPMA provides information only on the metal cation content present in a phase, but fails to distinguish the proportions of the cations of the same elements with different valences. Therefore, in the present study, for the purpose

of phase diagram construction, metallic molar ratio ($n_V/(n_{Mn}+n_V)$) is used as a composition variable.

2.2 Results and Discussions

Hereafter, the system investigated in the present study will be called the MnO-V_2O_3 system since both end-members in the system are MnO and V_2O_3, although other valencies of Mn and V may present. The phase diagrams derived from the experimental data are presented in Figure 1(a) (at P_{CO}/P_{CO_2} = 1), and Figure 1(b) (at P_{CO}/P_{CO_2} = 9), respectively. Calculated oxygen partial pressures using Factsage[3], [4] at each temperature are also specified in the figures. Solid lines in figures are phase boundaries determined by the experimental data obtained in the present study. Dashed lines are tentative phase boundaries (liquidus and solidus) due to lack of information above 1600°C. However, melting temperatures of pure MnO and pure V_2O_3, and limiting slope of liquidus[5] of pure MnO and pure V_2O_3 (shown as dotted lines) were taken into account in the drawing of the lines utilizing data (melting temperatures and enthalpies of fusion of MnO and V_2O_3, respectively) available in literature[1], [6]. Whether $(MnV_2O_4)_{s.s.}$ melts congruently or incongruently cannot be determined by the results obtained in the present study. Although Muan and Najjar[7] proposed a congruent melting behavior of $(MnV_2O_4)_{s.s.}$, no details were given to make such a conclusion. Further experimental verification is necessary.

Under the conditions investigated in the present study, the following phases have been observed: liquid oxide, MnO with limited solubility of V-oxide (halite, $(MnO)_{s.s.}$ hereafter), V_2O_3 with limited solubility of Mn-oxide (sesquioxide, $(V_2O_3)_{s.s.}$ hereafter), MnV_2O_4 with limited solubilities toward both MnO and V_2O_3 solid solutions (spinel, $(MnV_2O_4)_{s.s.}$ hereafter).

2.2.1 Phase diagram of the MnO-V_2O_3 system under P_{CO}/P_{CO_2} = 1

Phase diagram of the MnO-V_2O_3 system at P_{CO}/P_{CO_2} = 1 with metallic molar ratio ($n_V/(n_{Mn}+n_V)$) as compositional axis is shown in Figure 1(a). Solid symbols represent composition of $(MnV_2O_4)_{s.s}$ single phase measured by EPMA, while open symbols represent measured solubility limits of several phases. Mutual solubilities of V-oxide in MnO and Mn-oxide in V_2O_3 increase as the temperature increases. Maximum solubility of V-oxide in the MnO at 1576°C was found to be 9.2 mass pct. V_2O_3, and that of MnO in V_2O_3 at 1600°C is 4.3 mass pct. MnO.

The only intermediate phase observed in this phase diagram is $(MnV_2O_4)_{s.s.}$. According to XRD analysis, it was refined in the cubic $Fd\bar{3}m$ space group (a typical of spinel structure) with a lattice parameter of 8.5334Å ($n_V/(n_{Mn}+n_V)$=0.60), which is in agreement with 8.532Å[8] but slightly less than a recently reported value 8.5771Å[9]. This seems to be attributed to non-stoichiometric nature of the $(MnV_2O_4)_{s.s.}$. Stoichiometry of this MnV_2O_4 phase is close to a typical spinel type compounds (AB_2O_4 where A is divalent cation and B is trivalent cation) when it is in equilibrium with V_2O_3. On the other hand, it is observed that there is a noticeable non-stoichiometry toward MnO side, which increases as temperature increases.

As can be seen in the Figure 1(a), the liquid oxide phase was found to be in equilibrium with $(MnO)_{s.s.}$ or with $(MnV_2O_4)_{s.s.}$ at 1600°C. Compositions of the liquid oxide phase are very close to each other (31.6 mass pct. V_2O_3 in equilibrium with $(MnO)_{s.s.}$, and 33.0 mass pct. V_2O_3 in equilibrium with $(MnV_2O_4)_{s.s.}$). As it is also observed in the

present study that there is no liquid phase at 1576°C, the liquid oxide observed at 1600°C would undergo a eutectic reaction (liquid → $(MnO)_{s.s.}$ + $(MnV_2O_4)_{s.s.}$) between 1576°C and 1600°C, along with the eutectic composition between 31.6 to 33.0 mass pct. V_2O_3. However one should bear in mind that the proposed temperature and composition of the eutectic reaction is valid only under the oxygen partial pressure at the equimolar mixture of CO and CO_2.

2.2.2 Phase diagram of the MnO-V_2O_3 system under P_{CO}/P_{CO_2} = 9

Shown in Figure 1(b) is a phase diagram of the MnO-V_2O_3 system at P_{CO}/P_{CO_2} = 9. The gas mixture in this case gives approximately one hundred times lower oxygen partial pressure than the previous case shown in Figure 1(a), thus the system is under more reducing condition than that in the Figure 1(a). Most significant change observed in the Figure 1(b) compared to the Figure 1(a) is stable region of the $(MnV_2O_4)_{s.s.}$ phase. Non-stoichiometry of the $(MnV_2O_4)_{s.s.}$ in equilibrium with $(MnO)_{s.s.}$ was decreased, for example from 44 mass pct. MnO (P_{CO}/P_{CO_2} = 1) to 38 mass pct. MnO (P_{CO}/P_{CO_2} = 9) at 1500°C. Also, solubility of Mn-oxide in $(V_2O_3)_{s.s.}$ was also decreased. However, solubility of V-oxide in $(MnO)_{s.s.}$ increases as the oxygen partial pressure decreases.

Contrast to the observation in Figure 1(a), there was no liquid phase observed in this case (P_{CO}/P_{CO_2} = 9) up to 1600°C. It means that decreasing oxygen partial pressure increases stability of solid phases relative to liquid oxide phase composed of transition metals. It is partly attributed to the fact that the melting temperature of MnO (strictly speaking, a solid solution of $Mn^{2+}O$ with dissolved Mn^{3+}) in Mn-O system increases as oxygen partial pressure decreases due to decreasing Mn^{3+} in the MnO[1]. At present, however, it is not clear whether the melting temperature of $(MnV_2O_4)_{s.s.}$ increases or not as oxygen partial pressure decreases.

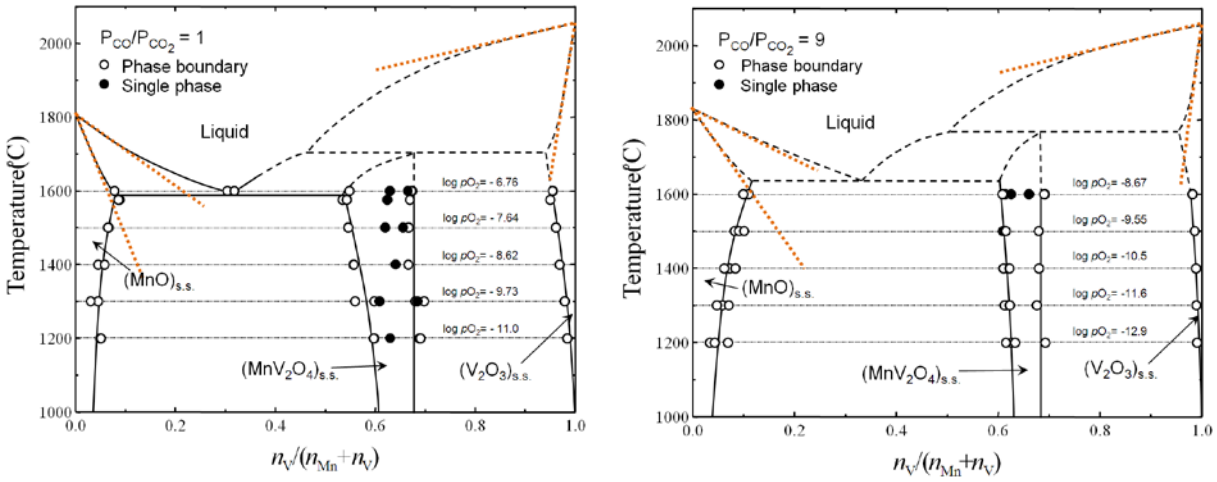

Figure 1. Phase diagram of the Mn-V-O system (a) under P_{CO}/P_{CO_2} = 1 and (b) under P_{CO}/P_{CO_2} = 9 measured in the present study. Dashed lines are tentatively drawn phase boundaries, according to limiting slopes of liquidus of MnO and V_2O_3 (dotted lines).

2.2.3 Phase diagram of the MnO-V_2O_3 system at 1500°C under different oxygen partial pressures

In order to determine the effect of oxygen partial pressure on the phase equilibria, additional experiments were conducted at 1500°C under H_2/CO_2 gas condition. The results together with those under CO/CO_2 gas mixtures at

1500°C are graphically presented in Figure 2. As described in Figure 1(a) and (b), solid lines are drawn based on the experimental data obtained in the present study, whereas dashed lines are only estimated to suggest tentative phase boundaries. As can be seen in the figure, increasing oxygen partial pressure increases solubility of Mn-oxide in $(MnV_2O_4)_{s.s.}$ which is in equilibrium with $(MnO)_{s.s.}$ and that of $(V_2O_3)_{s.s.}$ in equilibrium with $(MnV_2O_4)_{s.s.}$. Solubility of V-oxide in $(MnO)_{s.s.}$ is almost constant below pO_2 = ~10^{-9}, but slightly decreases above pO_2 = ~10^{-9}. Solubility of V-oxide in $(MnV_2O_4)_{s.s.}$ is almost constant above pO_2 = ~10^{-9}, but slightly increases below pO_2 = ~10^{-9}.

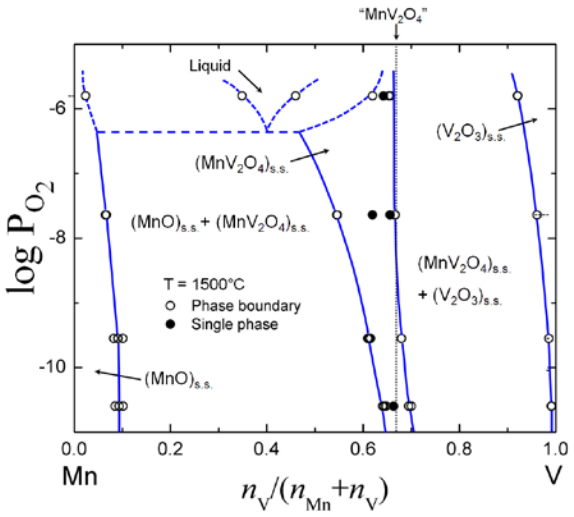

Figure 2. Effect of oxygen partial pressure on phase equilibria in the Mn-V-O system at 1500°C. Composition and oxygen partial pressure of a eutectic reaection (liquid → $(MnO)_{s.s.}$ + $(MnV_2O_4)_{s.s.}$) are only tentative, thus phase boundaries near the eutectic points are shown as dashed lines.

2.2.4 Non-stoichiometry of $(MnV_2O_4)_{s.s.}$

Since Mn and V are both transition metals, it is possible for those metals to have various valence states. Increasing solubility of Mn-oxide in $(MnV_2O_4)_{s.s.}$ in equilibrium with $(MnO)_{s.s.}$ is thought to be a result of Mn oxidation from divalent (Mn^{2+}) to trivalent (Mn^{3+}). Increasing the oxygen potential on MnO results in formation of Mn_3O_4 ($3MnO + 1/2O_2 = Mn_3O_4$) which is also cubic spinel at this temperature. Also, the same crystal structure of Mn_3O_4 and MnV_2O_4 suggests that those different spinel phases could make a solid solution whose solubility limit expands toward MnO side. Therefore, increasing the oxygen partial pressure results in the oxidation of Mn, and consequently results in increasing the solubility of Mn-oxide in the $(MnV_2O_4)_{s.s.}$. Similar types of Mn-oxide solubility in other spinel phases ($MnFe_2O_4$-Mn_3O_4, $MnAl_2O_4$-Mn_3O_4, $MnCr_2O_4$-Mn_3O_4, *etc.*) under relatively high oxygen partial pressure may be found[10].

Increasing the solubility of V-oxide in $(MnV_2O_4)_{s.s.}$ in equilibrium with $(V_2O_3)_{s.s.}$ by decreasing the oxygen partial pressure below pO_2 = ~10^{-9} may be attributed to V-oxide dissolution in the $(MnV_2O_4)_{s.s.}$ through reduction of V from trivalent (V^{3+}) to divalent (V^{2+}). A tentative description of the dissolution may be proposed as dissolution of a hypothetical "V_3O_4" in MnV_2O_4, although there is no report on the stable form of vanadium spinel phase ($V_1^{2+}V_2^{3+}O_4$). Other type of the V-oxide dissolution may be proposed such as the case of Al_2O_3 dissolution in $MgAl_2O_4$ spinel where

the Al_2O_3 dissolves in the form of γ-$Al_2^{3+}O_3$ ($Al_{\frac{8}{3}}^{3+}O_4$ with the spinel structure)[11]. However, if this is true, then solubility of the V-oxide would not be affected by the oxygen partial pressure because V has single valence state. This is contradiction to the observation in the present study. Therefore, the V-oxide solubility is likely to be a result of V reduction as described above.

It has been known that MnV_2O_4 has a normal cation distribution in which V is located mainly on the octahedral site[12]. The recent study by Pannunzio-Miner *et al.*[9] on structural information of MnV_2O_4 reported that the MnV_2O_4 has the crystallographic formula of $(Mn_{0.75}^{2+}V_{0.25}^{3+})^T(Mn_{0.25}^{2+}V_{1.75}^{3+})^O O_4$. This structural formula containing only Mn^{2+} and V^{3+} may be valid for the stoichiometric MnV_2O_4 under a certain oxygen partial pressure. However, according to the result obtained in the present study, under low oxygen partial pressures, the above formula cannot explain non-stoichiometry toward V-rich side, which requires either reduction of V^{3+} or oxidation of Mn^{3+} in order to keep electroneutrality (the latter is unlikely, of course). By considering:

a) Structural information of cubic Mn_3O_4 proposed by Dorris and Mason[13] and one of the present authors[1]
b) The discussions made in this section about V^{2+}
c) Preference of larger cation for tetrahedral site in a spinel structure[14] (ionic radius of V^{2+} is 0.79Å and that of V^{3+} is 0.64Å[15])

the following structure may be proposed for $(MnV_2O_4)_{s.s.}$:

$$(Mn^{2+}, V^{2+})^T\ (Mn^{2+}, Mn^{3+}, Mn^{4+}, V^{3+}, Va)_{2-x}^O\ O_4 \tag{2.1}$$

where the superscript “T” and “O” stands for tetrahedral and octahedral site in a fcc structure of spinel, respectively. “Va” means vacancy which resides in the octahedral site.

2.2.5 Solubilities in $(MnO)_{s.s.}$ and $(V_2O_3)_{s.s.}$

Solubility of Mn-oxide in $(V_2O_3)_{s.s.}$ increases as the oxygen partial pressure increases. Mn-oxide may dissolve as MnO (Mn^{2+}) and / or $MnO_{1.5}$ (Mn^{3+}). However, the former case (divalent cation in hexagonal corundum structure) is quite rare. Moreover, the increase of solubility of Mn-oxide by increasing oxygen partial pressure implies a stabilization of Mn^{3+} in the $(V_2O_3)_{s.s.}$. According to previous literatures[16], [17], V_2O_3 has a limited non-stoichiometry in V-O binary system toward O side. Therefore, the following structure of $(V_2O_3)_{s.s.}$ in the Mn-V-O system may be proposed (major cation in boldface).

$$(\mathbf{V}^{3+}, Mn^{3+}, V^{4+})_2\ O_{3+y} \tag{2.2}$$

Solubity of V-oxide in $(MnO)_{s.s.}$ decreases as the oxygen partial pressure increases. V-oxide may dissolve as VO (V^{2+}), $VO_{1.5}$ (V^{3+}) or other forms of higher valency states. However, decreasing the solubility by increasing the oxygen partial pressure implies that V prefers to be in a reduced form (lower valency), probably as V^{2+}. It is well known that MnO in Mn-O system has a considerable non-stochiometry toward O side by dissolving Mn^{3+}. Therefore the following structure for the $(MnO)_{s.s.}$ in the Mn-V-O system may be proposed (major cation in boldface).

$$(\mathbf{Mn}^{2+}, V^{2+}, Mn^{3+})_{1-z}\ O \tag{2.3}$$

3. Gibbs energy of formation of the MnV_2O_4 spinel phase

3.1 Experimental principle

A chemical reaction for the MnV_2O_4 spinel formation from its constituent oxide phases can be written as the following equation.

$$MnO(s) + V_2O_3(s) = MnV_2O_4(s) \qquad \Delta G^{o}_{f,MnV_2O_4} \tag{3.1}$$

The equation (3.1) can be derived by combining the three reactions below:

$$\underline{Mn}\ (\text{dissolved in metal}) + 2\underline{V}\ (\text{dissolved in metal}) + 4\underline{O}\ (\text{dissolved in metal}) = MnV_2O_4(s) \qquad \Delta G^{o}_{2} \tag{3.2}$$

$$MnO(s) = \underline{Mn} + \underline{O}\ (\text{dissolved in metal}) \qquad \Delta G^{o}_{3} \tag{3.3}$$

$$V_2O_3(s) = 2\underline{V} + 3\underline{O}\ (\text{dissolved in metal}) \qquad \Delta G^{o}_{4} \tag{3.4}$$

Therefore, the standard Gibbs free energy of formation of MnV_2O_4 solid solution from its constituent oxide phases (MnO and V_2O_3), $\Delta G^{o}_{f,MnV_2O_4}$, can be written as:

$$\Delta G^{o}_{f,MnV_2O_4} = \Delta G^{o}_{2} + \Delta G^{o}_{3} + \Delta G^{o}_{4} \tag{3.5}$$

where ΔG^{o}_{2}, ΔG^{o}_{3} and ΔG^{o}_{4} are the standard Gibbs free energy changes of the reactions (3.2), (3.3) and (3.4) respectively. With thermodynamic data of manganese, vanadium and oxygen in molten steel already available (ΔG^{o}_{3} and ΔG^{o}_{4}), the value of $\Delta G^{o}_{f,MnV_2O_4}$ can be obtained by investigating ΔG^{o}_{2} experimentally (see Table 1).

The standard Gibbs free energy change of the reaction (3.2) could also be written as:

$$\Delta G^{o}_{2} = -RT \ln\left(\frac{a_{MnV_2O_4}}{a_{\underline{Mn}} \cdot a^{2}_{\underline{V}} \cdot a^{4}_{\underline{O}}}\right) \tag{3.6}$$

where $a_{MnV_2O_4}$ is the Raoultian activity of MnV_2O_4 with respect to pure solid MnV_2O_4 as the standard state and all other a_i are the activities of component *i* with respect to 1 mass% in liquid metal as the standard state. Using Henrian activity coefficient with Wagner's first order interaction parameters for Mn, V and O, the activities in the above equation (3.6) could be calculated by measuring the composition of each component in the molten metal equilibrated with MnV_2O_4 crucible under controlled atmosphere:

$$\Delta G^{o}_{2} = -RT \ln\left(\frac{1}{\left(f_{\underline{Mn}}[\%Mn]\right)\cdot\left(f_{\underline{V}}[\%V]\right)^{2}\cdot\left(f_{\underline{O}}[\%O]\right)^{4}}\right) \tag{3.7}$$

$$\log f_{\underline{Mn}} = e^{Mn}_{Mn}[\%Mn] + e^{V}_{Mn}[\%V] + e^{O}_{Mn}[\%O] \tag{3.8}$$

$$\log f_{\underline{V}} = e^{V}_{V}[\%V] + e^{Mn}_{V}[\%Mn] + e^{O}_{V}[\%O] \tag{3.9}$$

$$\log f_{\underline{O}} = e^{O}_{O}[\%O] + e^{Mn}_{O}[\%Mn] + e^{V}_{O}[\%V] \tag{3.10}$$

where $f_{\underline{i}}$ and e^{j}_{i} represent activity coefficient of component i, and Wagner interaction parameter representing interaction between component *i* and *j* in liquid metal.

In the present study, liquid metal was supposed to be in equilibrium with MnV_2O_4. However, as shown in Sec. 2, it is not easy to keep a pure stoichiometric MnV_2O_4 in the experiments due to its own non-stoichiometry. Therefore, in the

present study, it is considered that "MnV_2O_4 saturated either by MnO or by V_2O_3" is the standard state of the reaction (3.1), and crucibles made of a mixure of MnV_2O_4 and MnO (or MnV_2O_4 and V_2O_3) were employed, thereby activity of MnV_2O_4 in the equation (3.6) will be unity for each crucible.

For the liquid metal to be equilibrated with the crucible, liquid iron and liquid copper were chosen. When liquid iron is used, corresponding interaction parameters were well documented and shown in Table 1. However, when the liquid Cu was introduced as the solvent in Cu-Mn-V-O system, the reported values of activity coefficients and interaction parameters in liquid copper obtained from experimental data were not applicable in the present study due to the different temperature range. Most of the thermodynamic properties from experimental data in liquid copper were collected and well-compilated by Sigworth and Elliott[18] but the applicable temperature range of the interaction coefficients and activity coefficient values for manganese is limited from 1100°C to 1240°C which is very low to introduce them in the present study. Tanahashi *et al.*[19] measured standard Gibbs free energy of formation of $MnCr_2O_4$ solid solution (MnO-saturated) at 1600°C using chemical equilibrium technique in liquid Cu system. They used the estimated γ°_{Mn} value calculated from the reported values of γ°_{Mn} at 1244°C by approximating the Cu-Mn system as the regular solution but the temperature difference between them is more than 300°C, which may not be a reasonable approach. In addition, the activity coefficient and interaction parameters of V directly measured by experimental study in the Cu-V binary system are not available.

Therefore, in the present study, the activity coefficients of Mn and V in the liquid copper were obtained by using excess Gibbs energies in the Cu-M systems from CALPHAD type thermodynamic optimizations, assuming that the interaction between Mn and V in the liquid copper may be negligible due to their low concentrations.[20],[21] Parameters used for the calculations are given in Table 2.

Using the activity coefficients of Mn and V determined by those parameters, the Gibbs energy of formation of MnV_2O_4 spinel phase in liquid Cu is obtained using the activity values of Mn and V, oxygen partial pressure calculated from the mixed ratio of H_2 and CO_2 gas, and several reaction equations for MnO and V_2O_3 formation as described below:

$$Mn\ (l) + 2V\ (l) + 2O_2\ (g) = MnV_2O_4\ (MnO \text{ or } V_2O_3\text{-satd.}) \qquad \Delta G^{o}_{11} \tag{3.11}$$

$$\Delta G^{o}_{11} = -\,RT \ln\left(\frac{a_{MnV_2O_4}}{a_{Mn} \cdot a_{V}^{2} \cdot p_{O_2}^{2}}\right) \tag{3.12}$$

$$MnO(s) = Mn(l) + 1/2O_2\ (g) \qquad \Delta G^{o}_{13} \tag{3.13}$$

$$V_2O_3(s) = 2V(l) + 3/2O_2(g) \qquad \Delta G^{o}_{14} \tag{3.14}$$

$$\Delta G^{o}_{f,MnV_2O_4} = \Delta G^{o}_{11} + \Delta G^{o}_{13} + \Delta G^{o}_{14} \tag{3.15}$$

where $a_{MnV_2O_4}$ is the Raoultian activity of MnV_2O_4 with respect to MnV_2O_4 solid solution saturated by MnO or V_2O_3 as the standard state (the value of $a_{MnV_2O_4}$ will be 1), a_i is the activity of component *i* with respect to pure component in liquid as the standard state and p_{O_2} is the oxygen partial pressure determined by H_2/CO_2 mixed gas exerted in the system.

Table 1. Thermodynamic properties related to liquid steel melt used for determination of standard Gibbs free energy of formation of MnV_2O_4 spinel solid solution saturated with either MnO or V_2O_3.

(a) Standard Gibbs free energy changes of the component oxides in MnV_2O_4 spinel phase.

Standard Gibbs Free Energy Change			
Reaction	**$\triangle G°$(J)**	**Temp. Range (K)**	**Ref.**
$\underline{Mn} + \underline{O} = MnO(s)$	-284900 + 127.64T	1823-1973	[22]
$2\underline{V} + 3\underline{O} = V_2O_3(s)$	-830700 + 337.0T	1823-1973	[22]

(b) Interaction parameters for Mn, V, and O

Interaction Parameter														
i	***j***	e_i^j	**Temp. Range (K)**	**Ref.**	***i***	***j***	e_i^j	**Temp. Range (K)**	**Ref.**	***i***	***j***	e_i^j	**Temp. Range (K)**	**Ref.**
	Mn	0	1823-1973	[22]		Mn	0.0056	1843			Mn	-0.021	1823-1973	
Mn	V	0.0057	1843	[23]	V	V	30/T-0.22	1823-1973	[22]	O	V	-1050/T+0.42	1823-1923	[22]
	O	-0.083	1823-1973	[22]		O	-3350/T+1.33	1823-1923			O	-1750/T+0.76	1823-1923	

Table 2. Thermodynamic properties related to liquid copper melt used for determination of standard Gibbs free energy of formation of MnV_2O_4 spinel solid solution saturated with either MnO or V_2O_3.

(a) Standard Gibbs free energy changes of the component oxides in MnV_2O_4 spinel phase.

Standard Gibbs Free Energy Change			
Reaction	**$\Delta G°$(J)**	**Temp. Range (K)**	**Ref.**
$Mn(l) + 1/2O_2(g) = MnO(s)$	-404630 + 86.74T	1600-2000	[19]
$2V(l) + 3/2O_2(g) = V_2O_3(s)$	-1248589 + 258.36T	298-2343	[24]

(b) Thermodynamic parameters of Cu-M binary systems.

System	**Phase**	**Parameter values**	**Ref.**
Cu-Mn	Liquid	Ω^L_{CuMn} = -10600 + 4.4T + (-19000 + 4.65T)(X_{Cu}-X_{Mn})	[20]
Cu-V	Liquid	Ω^L_{CuV} = 118298.01 - 38.49052T - 1137.38(X_{Cu}-X_{Mn})	[21]

3.2 Equilibrium experiments

Crucibles used in the present study were prepared by the present authors by sintering powder mixtures of MnO and V_2O_3 in order to ensure the liquid metal phase to be in equilibrium with both solid oxide phases (either MnV_2O_4/MnO or MnV_2O_4/V_2O_3). The sintered crucible was charged with appropriate amount of ferromanganese, ferrovanadium, FeO (chemical pure grade, JUNSEI CHEMICAL Co., Japan), and the electrolytic steel when the liquid metal is liquid Fe. When liquid Cu is used for the liquid metal phase, appropriate amount of copper metal (99.997% purity, 3mm pellet type, RND Company, Korea), manganese chip (99.9% KOJUNDO CHEMICAL Co., Japan) and vanadium powder (99.9% purity, LTS Chemical Inc., The United States) were used. This MnV_2O_4 crucibles filled with samples were carried in a protective MgO crucible and placed in the uniform temperature zone of a vertical $LaCrO_3$ resistance furnace at 1550°. The oxygen partial pressure was controlled using H_2 (99.99% purity) and CO_2 (99.5% purity) gas mixture (P_{H_2}/P_{CO_2} = 9) when liquid Cu was used. When liquid Fe was used, purified Ar gas ($\log pO_2$ = ~10^{-12}) stream was flown

over the sample. After equilibration, the whole specimen was quenched into cold water and cut into several pieces to analyze the equilibrium composition of Mn, V, and O dissolved in the liquid melt. Manganese and vanadium concentrations were analyzed by ICP-AES and oxygen by LECO combustion analysis (LECO® TC-300). Also, the samples of each crucible were mounted and subjected into electron probe microanalysis (EPMA) for the identification of equilibrium phases and measurement of composition of each oxide phase in equilibrium.

3.3 Results and discussions

3.3.1 The standard Gibbs energy of formation of the MnV_2O_4 spinel phase saturated with either MnO or V_2O_3

Using the equilbrium compositions of Mn, V, and O dissolved in the liquid melts and the thermodynamic properties in Table 1 and 2, the standard Gibbs free energy of formation of MnV_2O_4 saturated with either MnO or V_2O_3 was obtained as described in Sec. 3.1. No contamination of oxide phases in the crucible by Fe-oxide was observed by EPMA.

The determined values of $\Delta G^{o}_{f,MnV_2O_4}$ at 1550°C are plotted in Figure 3 against the oxygen partial pressure which was calculated from the equilibrium composition of Mn, V and O in liquid steel using the following equation and Equation 3.10:

$$\underline{O}\ (\text{mass\% in molten steel}) = 1/2O_2(g),\ \Delta G°(J) = -113700 - 5.83T \qquad (3.16)$$

For $\log(pO_2)$ in liquid Cu, it was calculated from the mixed gas (P_{H_2}:P_{CO_2}=9:1) and temperature (1550°C) by using thermodynamic software.[3] Regardless of the type of MnV_2O_4, the standard Gibbs energy of formation obtained in this study are independent of the oxygen partial pressure within the $\log(p_{O_2})$ range from -11.7 to -10.2. The standard Gibbs enerfy of formation of the following reactions at 1550°C were determined to be:

$$MnO(s) + V_2O_3(s) = MnV_2O_4(\textbf{MnO-satd.}):\ \Delta G^{o}_{f,MnV_2O_4}(kJ) = \textbf{-31.4±2}$$
$$MnO(s) + V_2O_3(s) = MnV_2O_4(\textbf{V}_2\textbf{O}_3\textbf{-satd.}):\ \Delta G^{o}_{f,MnV_2O_4}(kJ) = \textbf{-38.2±2}$$

Regardless of metal phase used in the experiments, the obtained Gibbs energy of formation of MnV_2O_4 are in good agreement each other as shown in Figure 3. Averbukh *et al.*[25] reported equilibrium compositions of Mn, V, and O dissolved in liquid steel at 1600°C, which could produce $\Delta G^{o}_{f,MnV_2O_4}$ values under the assumption that MnV_2O_4 spinel solid solution was formed in their experiments. Even though the oxide phases in equilibrium with the liquid steel in their experiments were not clearly identified in the literature, an inclusion stability diagram constructed with the experimental data in the present study (Figure 4) suggests that some data well-fitted on the MnV_2O_4-V_2O_3 boundary curve. It means that their experiments were conducted in MnV_2O_4/V_2O_3 co-saturation condition. In this manner, the selected values of standard Gibbs energy of formation of MnV_2O_4 from their research are also plotted on the Figure 3 (diamond symbol) to figure out the effect of temperature on the $\Delta G^{o}_{f,MnV_2O_4}$ values. However, very strong dependency on p_{O_2} of the Gibbs energy was observed, which is not general.

3.4.2 The stability diagram in the Fe-Mn-V-O system

Figure 4 shows the stability diagram constructed by plotting the experimental data obtained in the present study. Some of experimental data obtained by Averbukh *et al.*[25] are in good agreement with the present experimental work of

the MnV_2O_4-V_2O_3 phase boundary. The experimental results in liquid Fe-MnV_2O_4 (MnO-satd.)-H_2/CO_2 mixed gas system which contains Fe-oxide in the oxide phases are also well-fitted on the MnO-MnV_2O_4 phase boundary. From Figure 4, the type of oxide inclusion possible to be formed in a certain steel composition at 1550°C could be predicted.

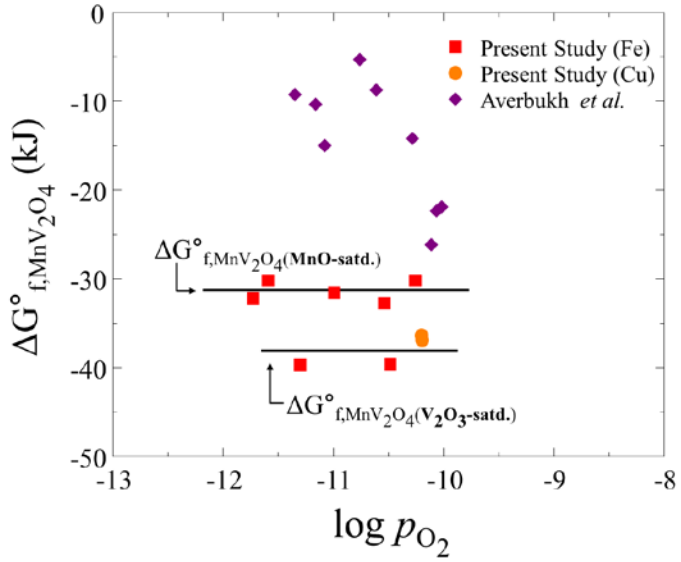

Figure 3. Effect of oxygen partial pressure on $\Delta G^{o}_{f,MnV_2O_4}$ from its constituent oxides (MnO and V_2O_3) in the present study at 1550°C.

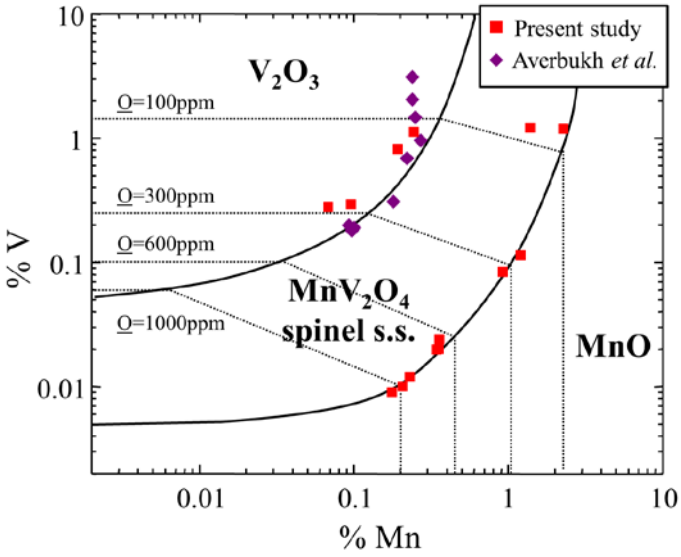

Figure 4. The stability diagram in the Fe-Mn-V-O system at 1550°C based on the experimental data in the present study and the reported data at 1600°C by Averbukh *et al.*[25] Iso-oxygen lines were estimated based on the equilibrium composition of oxygen dissolved in liquid steel.

4. Conclusion

Thermodynamic investigation on the Mn-V-O oxide system and MnV_2O_4 solid solution under the steelmaking condition was conducted with two main topics, phase equilibria in the Mn-V-O system and thermodynamic investigation on the MnV_2O_4 spinel phase.

1) Phase equilibria in the Mn-V-O system under controlled atmosphere were investigated in the temperature range from 1200°C to 1600°C and in the range of log p_{O_2} from -6 to -13. The following phases were observed; liquid oxide, $(MnO)_{s.s.}$, $(V_2O_3)_{s.s.}$, and $(MnV_2O_4)_{s.s.}$. The $(MnV_2O_4)_{s.s.}$phase was confirmed to be the only intermediate phase.

2) Sub-solidus phase equilibria in the present system are found to be affected significantly by the oxygen partial pressure. From the effect of oxygen partial pressure on the sub-solidus phase equilibria, possible structural forms of solid solutions were proposed:

   (a) Spinel: $(MnV_2O_4)_{s.s.}$ $(Mn^{2+}, V^{2+})^T\ (Mn^{2+}, Mn^{3+}, Mn^{4+}, V^{3+}, Va)^O_{2-x}\ O_4$

   (b) Sesquioxide: $(V_2O_3)_{s.s.}$ $(\mathbf{V}^{3+}, Mn^{3+}, V^{4+})_2O_{3+y}$

   (c) Halite: $(MnO)_{s.s.}$ $(\mathbf{Mn}^{2+}, V^{2+}, Mn^{3+})_{1-z}O$

3) Solid phases became less stable as the oxygen partial pressure increases. Under the relatively high oxygen partial pressure (P_{CO}/P_{CO_2} = 1), there was a eutectic reaction (liquid → $(MnO)_{s.s.}$ + $(MnV_2O_4)_{s.s.}$) along with the eutectic composition between 31.6 to 33.0 mass pct. V_2O_3 between 1576°C and 1600°C. Unfortunately any liquid oxide between $(MnV_2O_4)_{s.s.}$ and $(V_2O_3)_{s.s.}$ could not be observed due to the high temperature characteristic.

4) Using the equilbrium compositions of Mn, V, and O dissolved in the liquid melts in equilibrium with MnV_2O_4 spinel phase (either saturated with MnO or V_2O_3), and the thermodynamic properties available in literatures, the standard Gibbs free energy of formation of MnV_2O_4 saturated with either MnO or V_2O_3 was determined for the following equations:

$$MnO(s) + V_2O_3(s) = MnV_2O_4\ (\mathbf{MnO\text{-}satd.}):\ \Delta G^{o}_{f,MnV_2O_4}(kJ) = \mathbf{-31.4\pm2}$$
$$MnO(s) + V_2O_3(s) = MnV_2O_4\ (\mathbf{V_2O_3\text{-}satd.}):\ \Delta G^{o}_{f,MnV_2O_4}(kJ) = \mathbf{-38.2\pm2}$$

5) From the equilibrium compositions of the samples using liquid steel melt, the stability diagram in the Fe-Mn-V-O system was constructed. The inclusion stability diagram constructed in the present study could be used to predict the formation of possible oxide inclusions under relevant condition in the steelmaking.

Acknowledgement

This work was financially supported by POSCO Ltd. through Steel Innovation Program to Graduate Institute of Ferrous Technology, Pohang University of Science and Technology.

Reference

[1] Y.-B. Kang and I.-H. Jung, Thermodynamic Modeling of Pyrometallurgical Oxide Systems Containing Mn Oxides, Proceedings of the VIII International Conference on Molten Slags, Fluxes and Salts, Universidad de Concepción, Gecamin Ltd., 2009, pp. 460-471.

[2] M. Wakihara and T. Katsura, Thermodynamic Properties of the V_2O_3-V_4O_7 System at Temperatures from 1400 to 1700K, Metall. Trans. 1 (1970) 363-366.

[3] C.W. Bale, P. Chartrand, S.A. Decterov, G. Eriksson, K. Hack, R. Ben Mahfoud, J. Melançon, A.D. Pelton and S. Petersen, FactSage Thermochemical Software and Databases, Calphad 26 (2) (2002) 189-228.

[4] C.W. Bale, E. Bélisle, P. Chartrand, S.A. Decterov, G. Eriksson, K. Hack, I.-H. Jung, Y.-B. Kang, J. Melançon, A.D. Pelton, C. Robelin and S. Petersen, FactSage Thermochemical Software and Databases – Recent Developments, Calphad 33 (2) (2009) 295-311.

[5] A.D. Pelton, On the Slpoes of Phase Boundaries, Metal. Mater. Trans. A 19 (7) (1988) 1819-1825.

[6] M. W. Chase, NIST-JANAF Thermochemical Tables, 4th Edition, National Institute of Standards and Technology, Gaithersburg, Maryland, 20899-0001, 1998.

[7] A. Muan and M. Najjar, Vanadium Spinel Materials in the V_2O_3-MnO-SiO_2 System, United States Patent N o.5,086,029 (1992).

[8] A. Manthiram, Synthesis of Vanadium Spinels by Hydrogen Reduction of Oxide Precursors, Polyhedron 4 (1985) 967-970.

[9] E. Pannunzio-Miner, J.D. Paoli, R.Sánchez and R. Carbonio, Crystal and Magnetic Structure and Cation Distribution of $Mn_{2-x}V_{1+x}O_4$ Spinels, Mater. Res. Bull. 44 (7) (2009) 1586-1591.

[10] M. Kowalski, P. Spencer and D. Neuschütz, Slag Atlas-Ch.3, VDEh, 1995.

[11] A. Navrotsky, B. Wechsler, K. Geisinger and F. Seifert, Thermochemistry of $MgAl_2O_4$-$Al_{8/3}O_4$ Defect Spinels, J. Am. Ceram. Soc. 69 (5) (1986) 418-422.

[12] M. Zakrzewski, E. Burk, W. Lustenhouwer, Vuorelainenite, A New Spinel, and Associated Minerals from the Satra (Dovrstorp) Pyrite Deposit, Central Sweden, Can. Mineral. 20 (1982) 281-290.

[13] S. Dorris and T. Mason, Electrical Properties and Cation Valencies in Mn_3O_4, J. Am. Ceram. Soc. 71 (1988) 379-385.

[14] H.St.C. O'Neil and A. Navrotsky, Simple Spinels: Crystallographic Parameters, Cation Radii, Lattice Energies, and Cation Distribution, American Mineralogist 68 (1983) 181-194.

[15] R. Shannon, Revised Effective Ionic Radii and Systematic Studies of Interatomic Distances in Halides and Chalcogenides, Acta Cryst. A32 (1976) 751-767.

[16] K. Kosuge, The Phase Diagram and Phase Transition of the V_2O_3-V_2O_5 System, J. Phys. Chem. Solids 28 (1967) 1613-1621.

[17] H. Endo, M. Wakihara, M. Taniguchi, T. Katsura, Phase Equilibria in the V_2O_2-VO_2 System at High Temperatures, Bull. Chem. Soc. Jpn. 46 (1973) 2087-2090.

[18] G.K. Sigworth and J.F. Elliott, The Thermodynamics of Dilute Liquid Copper Alloys, Can. Metall.Q., 13 (1974), 455-460.

[19] M. Tanahashi, N. Furuta, T. Taniguchi, C. Yamauchi, and T. Fujisawa, Phase Equilibria of the MnO-SiO_2-CrO_x System at 1873K under Controlled Oxygen Partial Pressure, ISIJ int. 43 (2003) 7-13.

[20] H. Ohtani, H. Suda, and K. Ishida, Solid/Liquid Equilibria in Fe-Cu Based Ternary Systems, ISIJ int., 37 (1997), 211.

[21] M. Hämäläinen, K. Jääskeläinen, R. Luoma, M. Nuotio, P. Taskinen, and O.Teppo, A Thermodynamic Analysis of the Binary Alloy Systems Cu-Cr, Cu-Nb and Cu-V, Calphad, 14 (1990), 135.

[22] Steelmaking data sourcebook, Revised Ed., ed. By The Japan Society for the Promotion of Science, The 19th Committee on Steelmaking, Gordon and Breach Science Publishers, Montreux, 1984.

[23] K. Mukai and A. Uchida, Effect of Carbon, Cobalt, Nickel, Silicon, Titanium, and Vanadium on the Activity Coefficient of Manganese in Liquid Iron Alloy, Tetsu-to-Hagane (J. Iron Steel Inst. Jpn.), 60 (1974), 325-336, in Japanese.

[24] E.T. Turkdogan, Physical Chemistry of High Temperature Technology, Academic Press, New York (1980), 23.

[25] S.M. Averbukh, L.A. Smirnov, and S.I. Popel', Equilibrium of Vanadium and Manganese with Oxygen in Liquid Iron, Izv. Vuzov. Chern. Metallurgiya, 6 (1983) 1-3.